Reduced magnitude and shifted seasonality of CO$_2$ sink by experimental warming in a coastal wetland

Baoyu Sun [ID],[1,2,3] Liming Yan [ID],[1,4,6] Ming Jiang [ID],[1,4] Xinge Li,[3,5]
Guangxuan Han [ID],[3,5] and Jianyang Xia [ID][1,4]

[1]*State Key Laboratory of Estuarine and Coastal Research, Shanghai Key Lab for Urban Ecological Processes and Eco-Restoration, School of Ecological and Environmental Sciences, East China Normal University, Shanghai 200000 China*
[2]*Joint Translational Science and Technology Research Institute, East China Normal University and Haifa University, Shanghai 200000 China*
[3]*Key Laboratory of Coastal Zone Environmental Processes and Ecological Remediation, Yantai Institute of Coastal Zone Research, Chinese Academy of Sciences, Yantai 264000 China*
[4]*Research Center for Global Change and Ecological Forecasting, East China Normal University, Shanghai 200000 China*
[5]*University of Chinese Academy of Sciences, Beijing 100000 China*

Abstract. Coastal wetlands have the highest carbon sequestration rate per unit area among all unmanaged natural ecosystems. However, how the magnitude and seasonality of the CO$_2$ sink in coastal wetlands will respond to future climate warming remains unclear. Here, based on measurements of ecosystem CO$_2$ fluxes in a field experiment in the Yellow River Delta, we found that experimental warming (i.e., a 2.4°C increase in soil temperature) reduced net ecosystem productivity (NEP) by 23.7% across two growing seasons of 2017–2018. Such a reduction in NEP resulted from the greater decrease in gross primary productivity (GPP) than ecosystem respiration (ER) under warming. The negative warming effect on NEP mainly occurred in summer (−43.9%) but not in autumn (+61.3%), leading to a shifted NEP seasonality under warming. Further analyses showed that the warming effects on ecosystem CO$_2$ exchange were mainly controlled by soil salinity and its corresponding impacts on species composition. For example, warming increased soil salinity (+35.0%), reduced total aboveground biomass (−9.9%), and benefited the growth of plant species with high salt tolerance and late peak growth. To the best of our knowledge, this study provides the first experimental evidence on the reduced magnitude and shifted seasonality of CO$_2$ exchange under climate warming in coastal wetlands. These findings underscore the high vulnerability of wetland CO$_2$ sink in coastal regions under future climate change.

Key words: climate warming; coastal wetlands; ecosystem carbon fluxes; seasonality; soil salinity; species composition.

INTRODUCTION

Coastal wetlands play an important role in the sequestration and the long-term storage of carbon (C) from the atmosphere (Gabler et al. 2017). By storing carbon for millennia in sediments and transporting organic matter laterally to the ocean, vegetated coastal wetlands are significant natural carbon dioxide (CO$_2$) sinks in the biosphere (Gabler et al. 2017). However, how the C cycle in global coastal wetlands will respond to climate warming is largely unknown. For example, because coastal wetlands are located in transition zones between the land and ocean, it is unclear how soil salinity regulates the responses of the C processes under climate warming

(Baldwin et al. 2014). Also, plant phenology can quickly respond to the rising temperature (Charles and Dukes 2009) and the shifts of species composition consequently influence the seasonality of ecosystem productivity or C fluxes (Richardson et al. 2013). Thus, to better protect the ecological services of coastal wetlands, it is critical to better understand changes in both magnitude and seasonality of ecosystem CO$_2$ exchange under future climate warming.

Temperature is suggested as one of the most important factors in regulating CO$_2$ exchanges. Climate warming could reduce ecosystem productivity and CO$_2$ sequestration in semiarid or arid ecosystems because of its positive effect on evapotranspiration (Wu et al. 2011). On the contrary, climate warming usually positively influences plant growth and ecosystem productivity in inland freshwater wetlands (Mäkiranta et al. 2018). In coastal wetlands, however, the water-soluble salts in the deep soil can be transferred to the root zone and soil surface through

capillary rise and evapotranspiration (Yao and Yang 2010). The enhanced soil salinity in the root zone could suppress and even reverse the positive effect of climate warming on ecosystem productivity. On the one hand, the high salinity can cause additional abiotic stress on plant photosynthesis (Reef and Lovelock 2014, Najar et al. 2019). On the other hand, the high salinity stress can drive shifts in species composition by benefiting species with greater salinity tolerance, which may have lower productivity (Munns and Gilliham 2015, Zhang et al. 2017). Both of these salinity-driven impacts can alter the magnitude of ecosystem CO_2 exchange (Osland et al. 2018). Additionally, the interaction of elevated temperature and changed soil-water–salt dynamics can influence the seasonality of CO_2 fluxes. For example, leaf photosynthesis has been reduced during early summer but increased in autumn by experimental warming in Yellow River Delta (Sun et al. 2018). The role of soil salinity and its interplay with the vegetation community in coastal wetlands will complicate these seasonal patterns (Chu et al. 2018). Therefore, seasonal dynamics of abiotic and plant processes are important to clarify the underlying mechanisms of CO_2 exchanges under warming.

Numerous warming experiments have been carried out to explore the responses of magnitude and seasonality of ecosystem CO_2 fluxes. Those experiments have been conducted in the temperate steppe (Xia et al. 2009), mixed-grass prairie (Zhu et al. 2017), alpine meadow (Xu et al. 2016), and tundra ecosystems (Natali et al. 2011). Although previous experiments in coastal wetlands have also shown positive effects of warming on production (Gray and Mogg 2001, Charles and Dukes 2009, Gedan et al. 2011, Baldwin et al. 2014, Noyce et al. 2019), no study has reported the response of ecosystem CO_2 fluxes at the seasonal scale yet. In this study, a field warming experiment was conducted in a coastal wetland of Yellow River Delta. Three key questions were addressed: (1) Does climate warming shift the magnitude of the CO_2 sink in coastal wetlands? (2) Does climate warming influence the seasonality of the CO_2 sink? (3) What are the roles of abiotic factors and plant species composition in regulating the warming responses of ecosystem CO_2 fluxes?

MATERIALS AND METHODS

Site description

The study was conducted in Yellow River Delta Ecological Research Station of Coastal Wetlands (37°45′50″ N, 118°59′24″ E), Chinese Academy of Sciences. The experimental site has a warm-temperate and continental monsoon climate with distinctive seasons and a rainy summer. The mean annual temperature at this site is 12.9°C, with the mean seasonal temperature ranging from 26.7°C in summer to −2.8°C in winter. The average annual precipitation is 550–640 mm, nearly 70% of which falls between May and September. The average annual air temperature in this site has increased 1.7°C, and average annual precipitation has decreased 241.8 mm with the greatest decreases observed in summer from 1961 to 2015 (Han et al. 2018). The groundwater table in this region is shallow with an average depth of 1.1 m. The periodic surface ponding is often observed following heavy rainfall events. Due to the flat terrain and high groundwater table, the entire area is covered mainly by wet and saline soil. The natural vegetation in this area consists of salt-tolerant herbs, grasses, and shrubs. The most widespread vegetation types in the region are *Phragmites australis*, *Suaeda glauca*, *Suaeda salsa*, *Tamarix chinensis*, and *Imperata cylindrical*. The main growing season in this wetland ecosystem ranges from late April to late October.

Experimental design

The warming experiment was carried out in November 2014. A complete random block design was used with one treatment (warming) and replicated four times for a total of eight plots of 3×4 m^2 (four control plots and four warming plots). The distance between any two adjacent plots was 3 m. All the warmed plots were heated continuously by infrared heaters (Kalglo Electronics, Bethlehem, Pennsylvania, USA) suspended approximately 1.75 m above the ground from 1 November 2014. In each control plot, one "dummy" heater with the same dimensions as the infrared heater was suspended at the same height to mimic the shading effects of the heater. All the heaters under the warming treatments were set at a radiation output of approximately 1,600 W.

Meteorological measurements

In November 2014, eight 5TE sensors (Decagon Devices, Pullman, Washington, USA) were inserted at 10 cm depth of the soil in the center of each plot to monitor soil temperature, soil water content, and soil salt content. Data were automatically recorded at 2-h intervals by EM50 data loggers (Decagon Devices). Daily air temperature (HMP45C; Vaisala, Helsinki, Finland), precipitation (TE525 tipping bucket gauge; Texas Electronics, Dallas, Texas, USA), and photosynthetically active radiation (PAR; LI-190SB; Li-Cor, Lincoln, Nebraska, USA) were recorded automatically with an array of sensors installed 200 m away from the experimental site.

Ecosystem gas exchange measurements

Ecosystem gas exchanges were measured by a static-chamber method with an infrared gas analyzer (IRGA; LI-6400; LI-COR) attached to a transparent chamber (0.5 m diameter, 0.6 m height). Details about the static chamber can be found in previous studies (Xia et al. 2009). In April 2017, one circular aluminum frame (0.5 m diameter, 0.1 m height) was permanently inserted into the soil at 7 cm depth in each plot. One small

electric fan was fixed in the chamber and ran continuously to mix the air inside the chamber and 90-s consecutive recordings of CO_2 and H_2O concentrations were taken at 10-s intervals after steady-state conditions were achieved. CO_2 and H_2O flux rates were determined from the time courses of the concentrations to calculate net ecosystem productivity (NEP) and evapotranspiration (ET), respectively, according to the method of Xia et al. (2009). Following the measurement of NEP, the chamber was ventilated and reseated on the frame, and covered with an opaque cloth for the immediate measurement of ecosystem respiration (ER). Gross ecosystem primary productivity (GPP) was then calculated as the sum of NEP and ER. Positive or negative NEP (or GPP) values in this study represent net C uptake or release by the ecosystem, respectively. Seasonal gas exchange was usually measured two to three times a month on clear, sunny days between 09:00 and 11:00 from May to November in 2017 and 2018. Soil heterotrophic respiration (Rh) was also measured using a portable automated soil C flux system (Li-8100; Li-Cor) by deep collars that insert to 40-cm depth in the soil following some previous studies (Zou et al. 2018, Zhang et al. 2019).

Aboveground biomass

One permanent $1 \times 1 \ m^2$ quadrat was established in each plot in April 2015. Plant species composition and the number and height of every species in each quadrat were recorded twice each month from May to November during 2017 and 2018. In this study, a nondestructive method was used to estimate aboveground biomass by developing regression equations of biomass with the number and height of every species. Five calibration plots ($1 \times 1 \ m^2$) were set near our experimental plots in both years to include all the species occurred in our study. After measuring the number and height of each species in the experimental plots and in the calibration plots, we clipped the living aboveground biomass in the calibration plots and separated by species. Living tissues were separated from dead tissues, oven-dried at 70°C at least for 48 h, and weighed to determine dry biomass. We then developed regression equations of aboveground biomass (AB) with the number (N) and height (H) for each species. Good correlations were shown for all species in both 2017 and 2018. For example, the equations for *P. australis* (AB_{PA}) and *S. glauca* (AB_{SG}) in 2017 can be described as follows: $AB_{PA} = 1.18 \times N + 0.44 \times H - 27.04$ ($r^2 = 0.88$, $P < 0.01$); $AB_{SG} = 0.11 \times N \times EXP(0.033 \times H)$ ($r^2 = 0.94$, $P < 0.01$). Finally, the aboveground biomass of each species in the experimental plots was estimated by the corresponding equations.

Data analysis

The total growing season was divided into two periods, summer (1 May–5 August) and autumn (6 August–7 November). Repeated-measures ANOVAs were used to examine warming, year, season, and their interactions on soil temperature, soil moisture, soil salinity, aboveground biomass, and ecosystem gas fluxes in our study. Linear regressions were performed to explore the relationships of CO_2 fluxes with the abiotic (e.g., soil temperature, moisture, and salinity) and biotic variables (e.g., species' aboveground biomass and their relative ratio) at the seasonal scale. We then analyzed the interactive networks of factors (soil salinity, species' aboveground biomass, and their relative ratio), which regulated NEP in summer and autumn, respectively, by structural equation modeling (SEM). Relative effect strength for individual pathways was computed based on the relevant range standardization method (Grace et al. 2018). Note that as with all standardized partial effects, values are not constrained to fall between +1 and −1. All statistical analyses were conducted using SPSS17.0 (SPSS for Windows, Chicago, Illinois, USA).

RESULTS

Soil microclimate

The mean values of PAR were comparative between 2017 (380.8 $\mu mol \cdot m^{-2} \cdot s^{-1}$) and 2018 (356.7 $\mu mol \cdot m^{-2} \cdot s^{-1}$). Summer PAR was higher in 2017 than 2018 but there was no difference in autumn PAR between the two years (Fig. 1a, b). The mean air temperature during the growing season was 22.6°C in 2017 and 23.1°C in 2018. Total precipitation was 429 mm in 2017 and 443 mm in 2018. Episodic flooding often occurs in August with extremely high rainfall events. For example, there was a 42-mm and a 125-mm rainfall event in August of 2017 and 2018, respectively. The maximum flooding depths were 31.3 and 205.0 mm in 2017 and 2018, respectively. The duration of flooding events was 9 and 27 d in 2017 and 2018, respectively (Fig. 1c, d). Mean soil moisture and temperature in the control plots were similar between the two years (all $P > 0.05$, Table 1). However, the mean soil salinity in 2017 (4.0 dS/m) was slightly higher than that in 2018 (3.9 dS/m, $P = 0.01$, Table 1).

The results of RMANOVAs showed that warming significantly elevated soil temperature (+2.4°C, $P < 0.001$), moisture (+10.9%, $P = 0.001$), and salinity (+35.0%, $P = 0.001$) during the experimental period, with insignificant difference between 2017 and 2018 (all $P > 0.05$, Table 1). Across the whole year, greater stimulations of all abiotic factors were always found in summer than in autumn (Appendix S1: Table S1). For example, soil temperature was increased by 2.5°C in summer but by 2.3°C in autumn across the two years (Appendix S1: Table S1). Warming increased soil moisture by 9.8% and 21.8% in the summer of 2017 and 2018, respectively, but had an insignificant effect in autumn (all $P < 0.05$; Fig. 1g, h). During the two years, soil salinity was enhanced by
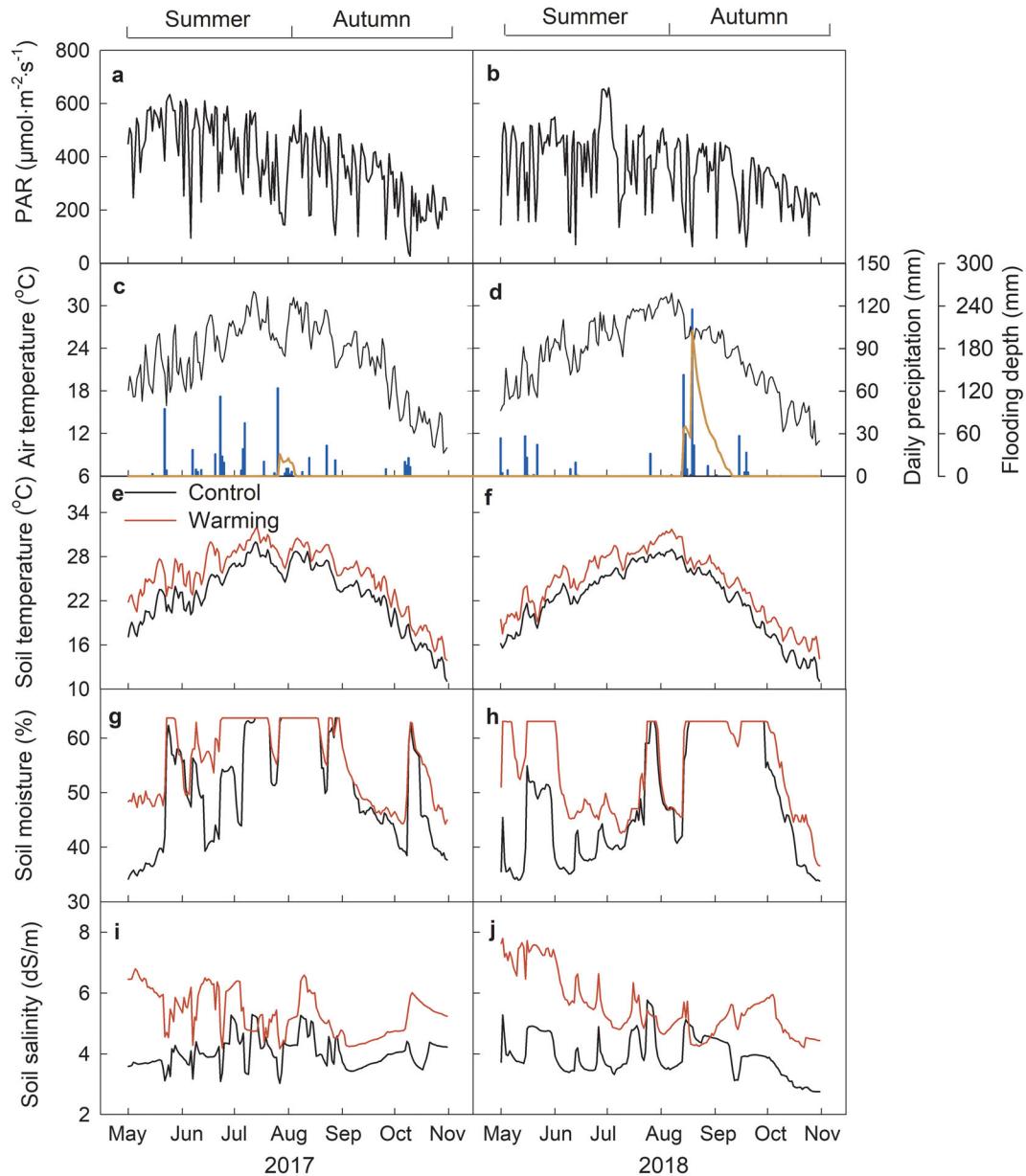
Fig. 1. (a, b) Daily photosynthetically active radiation (PAR). (c, d) Daily precipitation (bars) and daily mean air temperature (line) in 2017 and 2018. Daily variations in (e, f) soil temperature, (g, h) soil moisture, and (i, j) soil salinity at 10 cm depth in control and warming plots in 2017 and 2018 are also shown.

45.0% in summer but only 28.2% in autumn due to the flooding in August (all $P < 0.05$; Fig. 1i, j).

Seasonal variability in plant growth

The total aboveground biomass (AB_{total}) showed a pronounced seasonal pattern in both of the control and warmed plots, which raised from May, peaked in late August, and then declined (Fig. 2a, b). Warming showed a significant negative effect on AB_{total} (−9.9%; $P = 0.001$) over the two years (Appendix S1: Table S1).

Such a warming-induced reduction in AB_{total} was found in summer (27.6%) but not in autumn (Appendix S1: Table S1).

The peak aboveground biomass (ANPP) of *P. australis* (AB_{PA}) and *S. glauca* (AB_{SG}) accounts for 96.9% of the total ANPP in this ecosystem. However, *P. australis* had a fast growth period in summer, while the rapid growth of *S. glauca*. occurred in autumn. Thus, a greater ratio of AB_{PA} to AB_{SG} was observed in summer (5.0:1) than autumn (1.8:1). Across the two years, warming depressed AB_{PA} by 22.5% ($P < 0.001$) but increased

TABLE 1. Results (P values) of repeated-measures ANOVA on the effects of experimental warming (W), year (Y), season (S), and their interactions on soil temperature (T_{soil}), soil moisture (M_{soil}), soil salinity (S_{soil}), net ecosystem production (NEP), gross primary production (GPP), ecosystem respiration (ER), heterotrophic respiration (Rh), evapotranspiration (ET), aboveground biomass of community and species (AB$_{total}$, AB$_{PA}$, and AB$_{SG}$), and ratio of aboveground biomass of *Phragmites australis* and *Suaeda glauca*. (AB$_{PA}$/AB$_{SG}$).

| Source	T_{soil}	M_{soil}	S_{soil}	NEP	GPP	ER	Rh	ET	AB$_{total}$	AB$_{PA}$	AB$_{SG}$	AB$_{PA}$/ AB$_{SG}$
W	<0.001	0.001	0.001	<0.001	<0.001	<0.001	<0.001	0.002	<0.001	<0.001	<0.001	0.027
Y	0.325	0.304	0.010	<0.001	<0.001	0.966	<0.001	0.008	0.001	0.150	0.015	0.050
S	<0.001	0.029	<0.001	<0.001	<0.001	<0.001	<0.001	<0.001	<0.001	<0.001	<0.001	0.010
$W \times Y$	0.224	0.598	0.053	0.001	0.001	0.018	0.128	0.018	0.006	0.284	0.142	0.014
$W \times S$	0.003	0.017	0.010	0.007	<0.001	0.001	0.001	<0.001	<0.001	<0.001	<0.001	0.011
$Y \times S$	0.957	0.025	0.045	<0.001	<0.001	0.001	<0.001	<0.001	<0.001	<0.001	<0.001	0.001
$W \times Y \times S$	0.196	0.049	0.045	<0.001	<0.001	0.005	0.084	0.009	0.010	0.014	<0.001	0.001
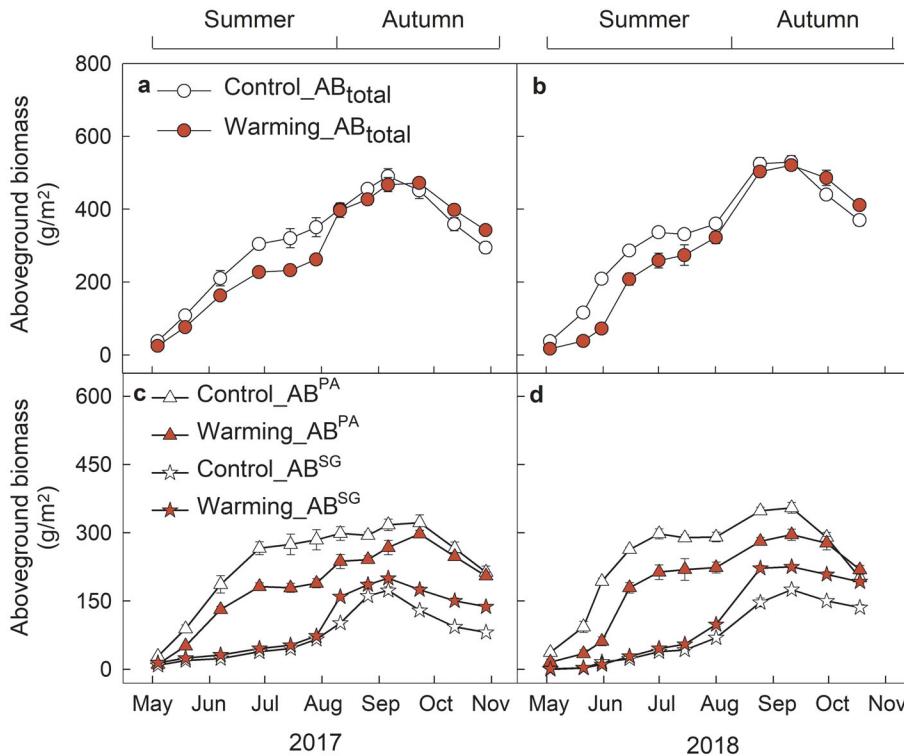
FIG. 2. Seasonal variations in aboveground biomass of community (AB$_{total}$), *Phragmites australis* (AB$_{PA}$), and *Suaeda glauca* (AB$_{SG}$) under warming and control plots in 2017 and 2018.

AB$_{SG}$ by 34.1% ($P < 0.001$; Table 1). The negative warming effect on AB$_{PA}$ was mainly observed in summer (−69.4 g/m^2) but the positive warming effect on AB$_{SG}$ occurred in autumn (+50.8 g/m^2; Appendix S1: Table S1). The RMANOVA results showed no difference in the warming response of either AB$_{PA}$ or AB$_{SG}$ between the two years (both $P > 0.05$).

Annual and seasonal ecosystem CO$_2$ fluxes

Ecosystem CO$_2$ fluxes (i.e., GPP, ER, and NEP) in the control plots showed significant seasonal dynamics in both growing seasons, which are consistent with the seasonal patterns of air temperature (Fig. 3). Rainfall also had an impact on the variations of CO$_2$ fluxes. For example, ecosystem CO$_2$ fluxes in August 2018 sharply decreased following a heavy rainfall event (Figs. 1d, 3b, d, f). NEP and GPP in 2018 were significantly higher than those in 2017, but there was no difference in ER between the two years (Table 1). The mean values of GPP, ER, and NEP in these two years were 38.8 ± 2.24, 16.7 ± 1.25, and 22.4 ± 1.68 g CO$_2$·m^{-2}·d^{-1}, respectively (Appendix S1: Table S1).

Warming significantly decreased all of GPP (−23.5%), ER (−26.9%), Rh (−24.5%), NEP (−23.7%), and ET (−20.8%) across the two years ($P < 0.001$, Table 1). The RMANOVA results showed that the effects of warming on CO_2 fluxes varied between years and seasons (all $P < 0.05$, Table 1). For example, warming decreased GPP, ER, and NEP by 28.1%, 34.9%, and 28.2%, respectively, in the summer of 2017 ($P < 0.01$; Fig. 3). In the

autumn, NEP was stimulated by 25.5% under warming, resulting from a decrease in ER and no response in GPP ($P < 0.01$; Fig. 4). Similarly, all of GPP, ER, and NEP were decreased in the summer of 2018 (−44.3%, −33.1%, and −50.9%) but increased (+115.1%, +57.7%, and +169.9%) in the autumn (all $P < 0.01$; Fig. 4). On average, warming decreased ER by 34.5% in summer and 13.1% in autumn. Warming significantly decreased
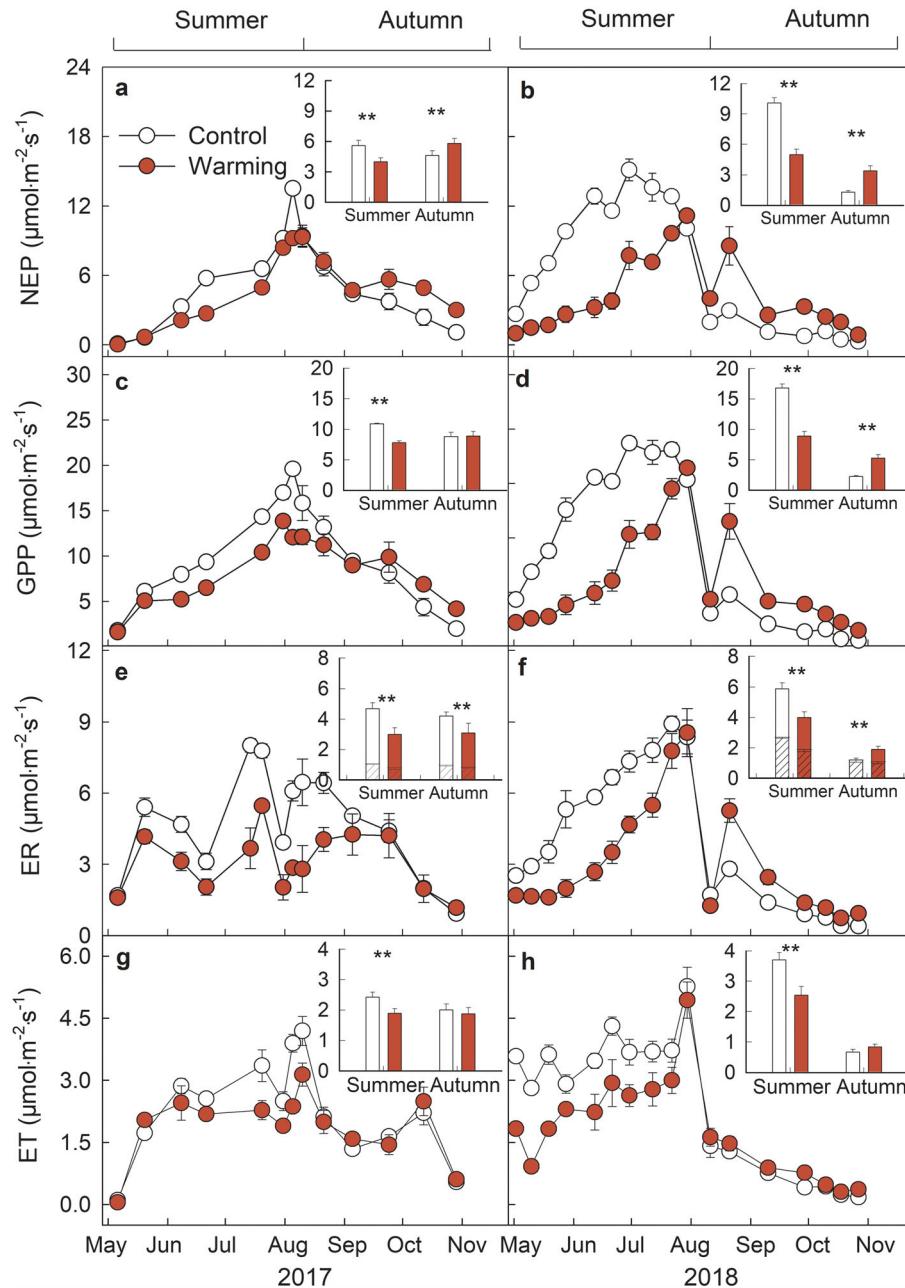

FIG. 3. Seasonal dynamics and mean values (±SE) of net ecosystem productivity (NEP), gross primary productivity (GPP), ecosystem respiration (ER), and evapotranspiration (ET) in the control and warming plots in 2017 and 2018. Insert panels show the mean values of ecosystem CO_2 fluxes in summer and autumn. ** $P < 0.01$.

Rh by 33.3% in summer but had no impact on Rh in autumn (Fig. 3e, f). However, the warming effects on GPP and NEP were negative in summer (NEP, −43.9%; GPP, −38.8%) but positive in autumn (NEP, +61.3%; GPP, +25.4%) across the two years (Appendix S1: Table S1, all $P < 0.05$). In addition, warming significantly decreased ET by 21.9% and 31.4% in the summer of 2017 and 2018, respectively, but had no effect in the autumn (Fig. 3g, h), leading to the reduced annual ET in both of 2017 (−15.5%) and 2018 (−25.1%).

Factors controlling ecosystem CO$_2$ fluxes under climate warming

Across the two years, GPP, ER, and NEP all increased with the increasing soil temperature (all $P < 0.01$). There was no significant relationship between the ecosystem CO$_2$ fluxes and other factors, including PAR, soil moisture, soil salinity, aboveground biomass of community (AB$_{total}$), and the ratio of AB$_{PA}$ to AB$_{SG}$ (AB$_{PA}$/AB$_{SG}$; all $P > 0.05$). The regression analysis showed that the effects of warming on CO$_2$ fluxes (i.e., ΔGPP and ΔER) had no significant relationship with the change in soil temperature or moisture (ΔT_{soil}, ΔM_{soil}; all $P > 0.05$). Across the two years, the warming-included changes in NEP and its two determinant fluxes (i.e., GPP and ER) all significantly and linearly correlated with the changes in plant biomass and AB$_{PA}$/AB$_{SG}$ (all $P < 0.001$; Fig. 5). The warming effects on soil salinity linearly and negatively influenced that on NEP ($P < 0.01$, Fig. 5c) and GPP ($P < 0.01$, Fig. 5f) but not ER ($P < 0.01$, Fig. 5i).

A structural equation model (SEM) was applied to explore the role of plant biomass change in regulating the warming impacts on NEP in different seasons. As shown in Fig. 6, the SEM model adequately fitted the data, by explaining 96% and 88% of the NEP variations in summer ($\chi^2 = 29.3$, $P = 0.059$, df = 8) and autumn ($\chi^2 = 36.3$, $P = 0.067$, df = 8), respectively. In summer,
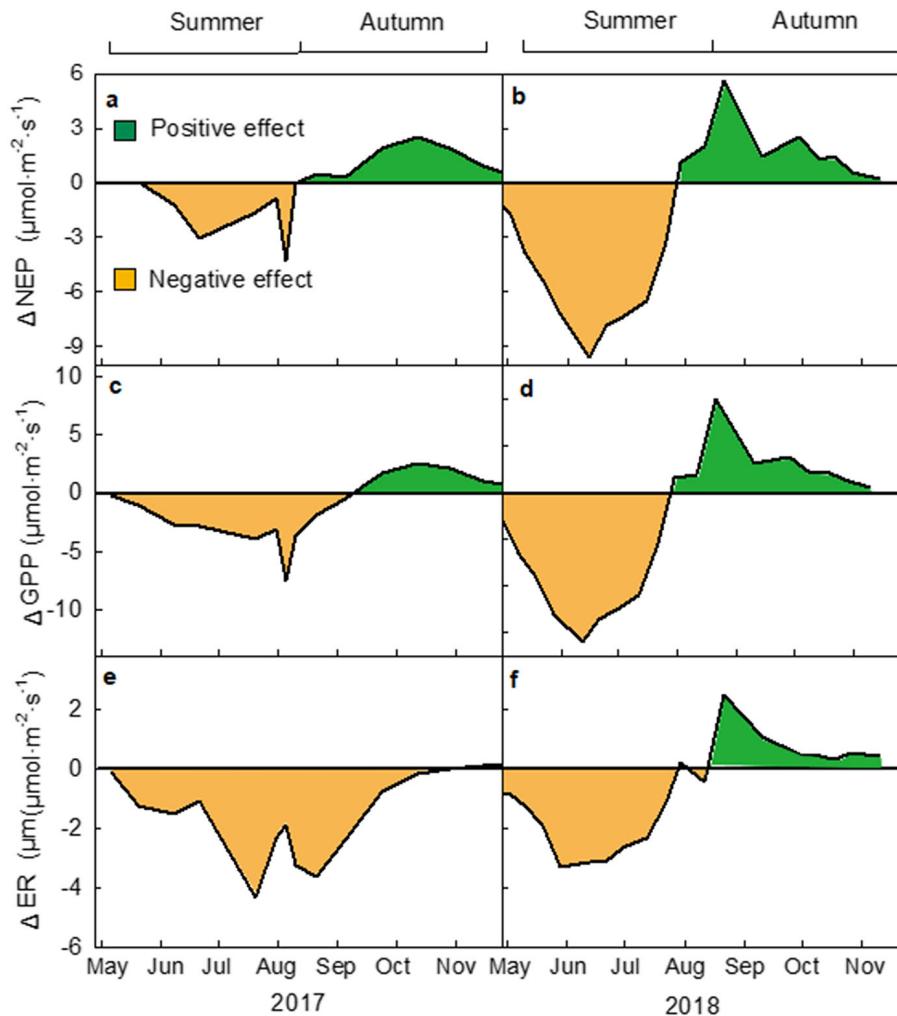

Fig. 4. Seasonal patterns of warming-induced changes in ecosystem C fluxes, net ecosystem production (ΔNEP), gross primary production (ΔGPP), and ecosystem respiration (ΔER).

warming decreased GPP ($P < 0.05$) largely via reducing AB_{total} (path coefficient -0.26, $P < 0.05$; Fig. 6a). In autumn, warming positively affected GPP (path coefficient 0.12, $P < 0.05$) by changing AB_{PA}/AB_{SG} (path coefficient -0.93, $P < 0.05$; Fig. 6b).

DISCUSSION

Seasonal patterns of ecosystem CO_2 exchanges

The magnitude of net ecosystem CO_2 uptake in this coastal wetland was 22.4 ± 1.67 g $CO_2 \cdot m^{-2} \cdot d^{-1}$ over the two growing seasons (Appendix S1: Table S1). This magnitude is comparable with the net ecosystem CO_2 sink in other wetlands, e.g., 20.9 g $CO_2 \cdot m^{-2} \cdot d^{-1}$ in a temperate cattail marsh (Dušek et al. 2009) and 28.9 g $CO_2 \cdot m^{-2} \cdot d^{-1}$ in a restored wetland (Knox et al. 2015). We found a higher NEP in 2018 than 2017 in this study (Table 1, Fig. 3), which is mainly driven by the larger aboveground biomass in 2017 than 2018 (Table 1, Fig. 2; Chu et al. 2019). On the seasonal scale, the seasonal changes in ecosystem CO_2 fluxes significantly depend on the changes in soil temperature (Appendix S1: Fig. S1), suggesting the important role of temperature change in regulating the seasonal dynamics of CO_2 fluxes. In addition, we found that the ecosystem CO_2 fluxes (i.e., GPP and ER) dropped sharply in

August 2018 (Fig. 3b, d, f). Such abrupt decreases were due to an extremely high rainfall event in August, leading to a flooding event from 14 August to 10 September. Flooding can limit photosynthesis and respiration of plants (Chu et al. 2018) and therefore lead to a sharply reduced ecosystem CO_2 fluxes in this region. These findings indicate that the seasonal changes in CO_2 fluxes in coastal wetlands are largely influenced by temperature and the redistribution of precipitation (Jimenez et al. 2012, Lu et al. 2017).

Reduced ecosystem CO_2 sink of coastal wetland by climate warming

Field observations along latitudinal gradients usually imply that warming can increase ecosystem productivity in tidal wetlands (Bouillon et al. 2008, Kirwan and Mudd 2012). This positive impact of warming on wetland CO_2 sink has also been confirmed by some recent manipulative experiments in salt marshes (Gray and Mogg 2001, Charles and Dukes 2009, Gedan et al. 2011, Baldwin et al. 2014). In this study, however, a negative warming effect on NEP has been observed over the two years (-23.7%, $P < 0.01$; Table 1 and Appendix S1: Table S1).

As shown by the regression analysis (Fig. 5) and the SEM approach (Fig. 6), the negative impacts of
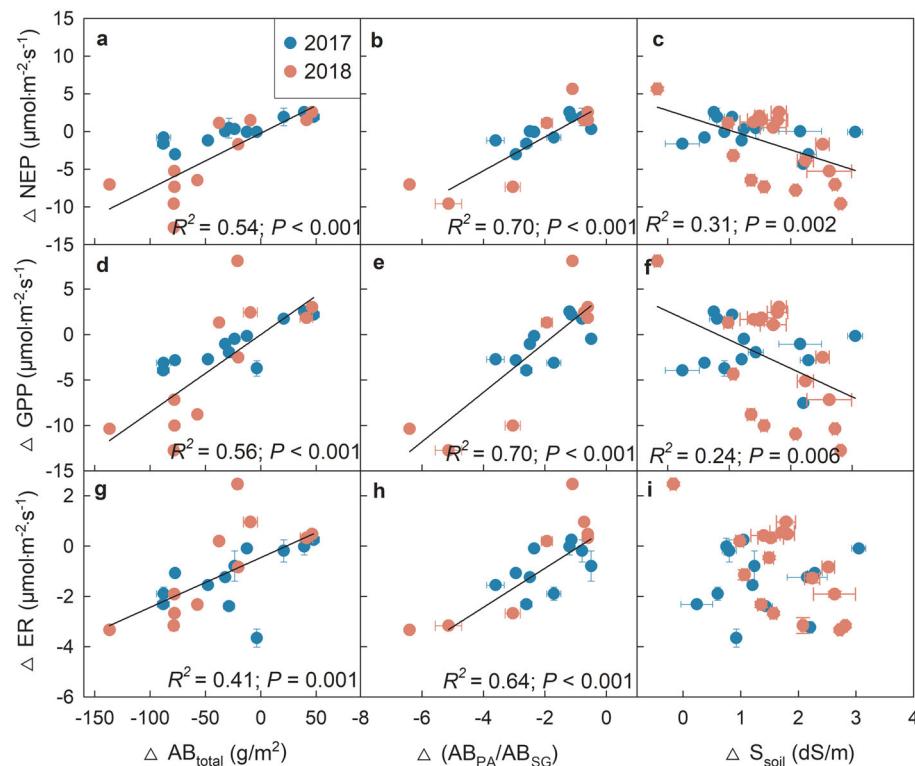

Fig. 5. Temporal correlations between warming-induced changes in CO_2 fluxes (i.e., ΔGPP, ΔNEP, and ΔER) and plant biomass (i.e., ΔAB_{total}, $\Delta(AB_{PA}/AB_{SG})$) and soil salinity (ΔS_{soil}) across the two experimental years. Values are mean $\pm$ SE.
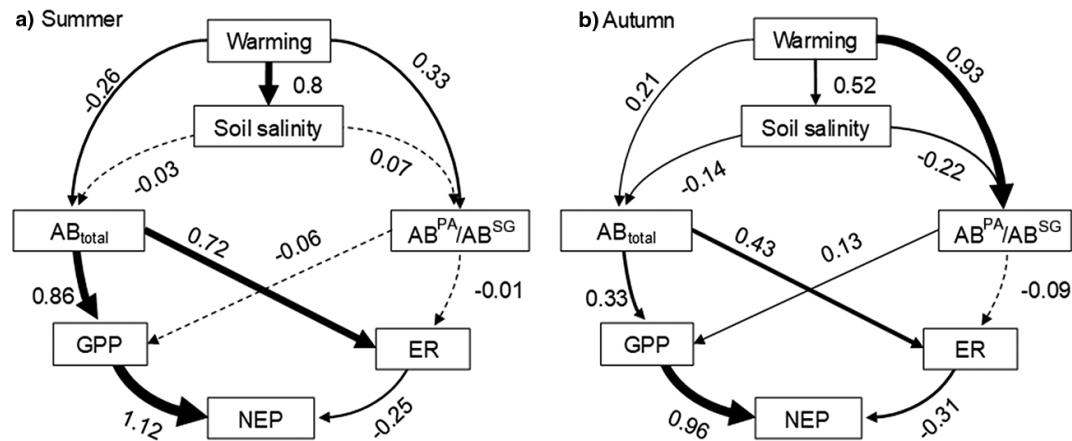
FIG. 6. Path diagrams showing the effects of abiotic and biotic factors on NEP during summer and autumn. Path arrow thickness reflects the strength of the relationship (thicker indicates stronger relationship). The value beside each arrow represents the standardized path coefficient. The solid lines shown were statistically significant ($P < 0.05$) and the dotted lines are shown were not significant ($P > 0.05$).

warming on NEP in this wetland were mainly driven by the increased soil salinity and decreased plant growth. The increase in soil salinity in the warming plots (+35.0%, Fig. 1i, j) mainly resulted from the enhanced evaporation by elevated temperature (Appendix S1: Fig. S2). The negative impact of high soil salinity on plant growth has been reported by many previous studies in wetlands (Greiner La Peyre et al. 2001, Osland et al. 2018). Thus, the reduced NEP under climate warming in this study is largely driven by reduced vegetation growth and GPP. Such a GPP-driven response of NEP to climate warming has also been reported in other ecosystems, such as a semiarid grassland (Xia et al. 2009). It is interesting that ER was also reduced by warming in this study (Fig. 3e, f). As shown in Appendix S1: Fig. S3, GPP and ER were significantly correlated in both summer and autumn seasons, suggesting that most of the decrease in ER can be explained by the decline in photosynthetic activity. In fact, a 24.5% reduction in heterotrophic respiration has been found under warming over 2017–2018 (Fig. 2e, f). The negative impacts of high soil salinity on heterotrophic respiration could result from the decreasing microbial activity and enzyme activity (Chambers et al. 2013).

The increase of soil salinity under warming shifts the wetland communities toward *S. glauca* from *P. australis*. Both *P. australis* and *S. glauca* are the dominant species in this ecosystem, while *S. glauca* shows a greater salinity tolerance (Zhang et al. 2017). In our study, the warming-induced increase in biomass of *S. glauca* was linearly correlated with the decrease in biomass of *P. australis* across the treatment blocks over the two years ($r^2 = 0.64$; $P = 0.010$, Appendix S1: Fig. S4). These results suggest that species replacement is occurring under warming in our experiment. The species replacement is important in regulating the responses of ecosystem CO$_2$ fluxes to climate warming (Gedan et al. 2011).

For example, the warming effect in a temperate steppe shifted from negative to positive owing to the changes in biomass proportion in grass and forb (Xia et al. 2009). Increasing CO$_2$ sequestration was observed in a tallgrass prairie due to the shift from C$_3$ to C$_4$ grasses under warming (Niu et al. 2013). In our study, we detected a positive relationship between warming-induced changes in NEP (i.e., ΔNEP) and the ratio of aboveground biomass of *P. australis* and *S. glauca* (i.e., ΔAB$_{PA}$/AB$_{SG}$; Fig. 5b). This finding suggests that the shift of *P. australis* to *S. glauca* under warming will alleviate the negative effect of warming on the ecosystem CO$_2$ exchanges.

Warming effects on the seasonality of ecosystem carbon exchanges

The warming effect on net carbon uptake (NEP) is negative in summer while positive in autumn in this study (Fig. 3). Previous studies in other regions have usually revealed that the decrease in soil moisture caused by warming plays a key role in regulating the seasonality of net carbon uptake (Zhu et al. 2017). However, in the Yellow River Delta, soil hydrological processes interacted with soil salinity in shaping the seasonality of CO$_2$ uptake (Chu et al. 2018). In our experiment, it was unexpected that soil moisture was stimulated by warming, especially in the summer. This finding is contrary to the reduced soil moisture by warming in most of the previous manipulative experiments (Xia et al. 2009, Natali et al. 2011). The increased soil moisture in warming plots could be explained by the decrease in evapotranspiration due to a declined canopy greenness (Ham and Knapp 1998) or earlier plant senescence (Zavaleta et al. 2003) under warming. In our study, evapotranspiration was significantly decreased in summer of 2017 (−21.9%) and 2018 (−31.4%; Fig. 3g, h). The stimulated biomass of *S. glauca* did not compensate for the declined

biomass of *P. australis* in summer, resulting in a decreasing total aboveground biomass under warming. In general, the opposite changes of soil moisture (Fig. 1g, h) and ecosystem CO_2 fluxes (Fig. 3) suggest that soil moisture is not the main factor in regulating the seasonal variability of ecosystem CO_2 fluxes under warming in this region.

The seasonality of warming effect on plant biomass is mainly controlled by the depression of AB_{PA} in summer and the stimulation of AB_{SG} in autumn (Fig. 2c, d). The different growth phenology and salinity tolerance between *P. australis* and *S. glauca* play important roles in driving such a seasonal pattern of the warming effect. The increased growth of *P. australis* by warming in autumn is largely due to the smaller increase in soil salinity under warming after the regular flooding in August than other periods (Fig. 1). The analytical results of the SEM model further show that the decrease of NEP in summer under warming is mostly driven by the decrease of plant biomass especially *P. australis*. However, the warming-induced increase of NEP in autumn mainly results from the enhanced growth of *S. glauca* (Fig. 6). The opposite warming responses between *P. australis* and *S. glauca* could be largely driven by the greater salinity tolerance of *S. glauca* than *P. australis*. Thus, the interactions between soil salinity and vegetation community have important impacts on the seasonality of carbon exchanges under future climate warming in the coastal wetlands.

Implications for the long-term response of coastal wetland CO_2 sink to climate warming

It should be noted that the experimental site of this study is located in a supratidal wetland of the Yellow River Delta. This means our experimental plots have a shallow and saline water table and beyond the reach of the tides (Zhong et al. 2013). Thus, there is a high uncertainty in making long-term predictions for coastal wetlands based on the short-term observations of species composition change under climate warming, as the warming effects on soil salinity would be regulated by rising sea level and the tides (Karim and Mimura 2008, Charles and Dukes 2009). Globally, only few manipulative experiments are located in coastal wetlands for studying the long-term ecological responses to global changes. In a long-term field experiment in a brackish wetland on the Chesapeake Bay, the stimulated shoot density and biomass production by elevated CO_2 in the first year (i.e., 1987) continued to 2016 (Lu et al. 2019). Also, the increased net ecosystem CO_2 uptake under elevated CO_2 was sustained from 1987 to 2004 in that experiment (Drake 2014). Therefore, we recommend more long-term experiments in coastal wetlands to explore whether or not the fast and short-term responses of species composition will continue in the long term.

Conclusion

This study provides experimental evidence for the reduced magnitude and shifted seasonality of ecosystem CO_2 exchange under warming in coastal wetlands. The reduced magnitude of the ecosystem CO_2 sink is driven by increased soil salinity and reduced vegetation growth under warming. The shifted seasonality of ecosystem CO_2 exchange under warming results from reduced NEP in summer but enhanced NEP in autumn, which is associated with the change of species composition. The shifting species composition under climate warming is jointly driven by the increasing soil salinity and the interspecific difference in salinity tolerance. These findings highlight that a continuous increase of salinity could increase the vulnerability of the wetland CO_2 sink in coastal regions under climate warming. It should be noted that this study is conducted in a supratidal wetland, where the an increase in soil salinity with warming is expected. Thus, our results have geographical limitations and the mechanism underlying warming is not universal across global coastal wetlands. In tidal wetlands, climate warming will not necessarily lead to higher soil salinity if rising seas and the accompanying tides flood the soil surface (Karim and Mimura 2008). However, if the precipitation is less than evaporation under future global warming, soil salinity is also predicted to increase in coastal tidal wetlands (Charles and Dukes 2009, Feher et al. 2017). Under such a climate scenario, the coupled thermal and salinity stresses under climate warming as reported in this study will be broadly applicable to coastal wetlands.

Literature Cited

Baldwin, A. H., K. Jensen, and M. Schönfeldt. 2014. Warming increases plant biomass and reduces diversity across continents, latitudes, and species migration scenarios in experimental wetland communities. Global Change Biology 20:835–850.

Bouillon, S., et al. 2008. Mangrove production and carbon sinks: a revision of global budget estimates. Global Biogeochemical Cycles 22:GB2013.

Chambers, L. C., T. Z. Osboorne, and K. R. Reddy. 2013. Effect of salinity-altering pulsing events on soil organic carbon loss along an intertidal wetland gradient: a laboratory experiment. Biogeochemistry 115:363–383.

Charles, H., and J. S. Dukes. 2009. Effects of warming and altered precipitation on plant and nutrient dynamics of a New England salt marsh. Ecological Applications 19:1758–1773.

Chu, X., G. Han, Q. Xing, J. Xia, B. Sun, X. Li, J. Yu, D. Li, and W. M. Song. 2019. Changes in plant biomass induced by

soil moisture variability drive interannual variation in the net ecosystem CO$_2$ exchange over a reclaimed coastal wetland. Agricultural and Forest Meteorology 264:138–148.

Chu, X., G. Han, Q. Xing, J. Xia, B. Sun, J. Yu, and D. Li. 2018. Dual effect of precipitation redistribution on net ecosystem CO$_2$ exchange of a coastal wetland in the Yellow River Delta. Agricultural and Forest Meteorology 249:286–296.

Drake, B. 2014. Rising sea level, temperature, and precipitation impact plant and ecosystem responses to elevated CO$_2$ on a Chesapeake Bay wetland: review of a 28-year study. Global Change Biology 20:3329–3343.

Dušek, J., H. Čížková, R. Czerný, K. Taufarová, M. Šmídová, and D. Janouš. 2009. Influence of summer flood on the net ecosystem exchange of CO$_2$ in a temperate sedge-grass marsh. Agricultural and Forest Meteorology 149:1524–1530.

Feher, L. C., et al. 2017. Linear and nonlinear effects of temperature and precipitation on ecosystem properties in tidal saline wetlands. Ecosphere 8:e01956.

Gabler, C. A., M. J. Osland, J. B. Grace, C. L. Stagg, R. H. Day, S. B. Hartley, N. M. Enwright, A. S. From, M. L. McCoy, and J. L. McLeod. 2017. Macroclimatic change expected to transform coastal wetland ecosystems this century. Nature Climate Change 7:142–147.

Gedan, K. B., A. H. Altieri, and M. D. Bertness. 2011. Uncertain future of New England salt marshes. Marine Ecology Progress Series 434:229–237.

Grace, J. B., D. Johnson, J. Lefcheck, and J. K. Byrnes. 2018. Quantifying relative importance: computing standardized effects in models with binary outcomes. Ecosphere 9:e02283.

Gray, A. J., and R. J. Mogg. 2001. Climate impacts on pioneer saltmarsh plants. Climate Research 8:105–112.

Greiner La Peyre, M. K., J. B. Grace, E. Hahn, and I. A. Mendelssohn. 2001. The importance of competition in regulating plant species abundance along a salinity gradient. Ecology 82:62–69.

Ham, J. M., and A. K. Knapp. 1998. Fluxes of CO$_2$, water vapor, and energy from a prairie ecosystem during the seasonal transition from carbon sink to carbon source. Agricultural and Forest Meteorology 89:1–14.

Han, G., B. Sun, X. Chu, Q. Xing, W. Song, and J. Xia. 2018. Precipitation events reduce soil respiration in a coastal wetland based on four-year continuous field measurements. Agricultural and Forest Meteorology 256–257:292–303.

Jimenez, K. L., G. Starr, C. L. Staudhammer, J. L. Schedlbauer, H. W. Loescher, S. L. Malone, and S. F. Oberbauer. 2012. Carbon dioxide exchange rates from short- and long-hydroperiod Everglades freshwater marsh. Journal of Geophysical Research Atmospheres 117:G04009.

Karim, M. F., and N. Mimura. 2008. Impacts of climate change and sea-level rise on cyclonic storm surge floods in Bangladesh. Global Environmental Change 18:490–500.

Kirwan, M. L., and S. M. Mudd. 2012. Response of salt-marsh carbon accumulation to climate change. Nature 489:550–553.

Knox, S. H., C. Sturtevant, J. H. Matthes, L. Koteen, J. Verfaillie, and D. Baldocchi. 2015. Agricultural peatland restoration: effects of land-use change on greenhouse gas (CO$_2$ and CH$_4$) fluxes in the Sacramento-San Joaquin Delta. Global Change Biology 21:750–765.

Lu, M., E. R. Herbert, J. Adam Langley, M. L. Kirwan, and J. Patrick Megonigal. 2019. Nitrogen status regulates morphological adaptation of marsh plants to elevated CO$_2$. Nature Climate Change 9:764–768.

Lu, W., J. Xiao, F. Liu, Y. Zhang, C. Liu, and G. Lin. 2017. Contrasting ecosystem CO$_2$ fluxes of inland and coastal wetlands: a meta-analysis of eddy covariance data. Global Change Biology 23:1180–1198.

Mäkiranta, P., R. Laiho, L. Mehtätalo, P. Straková, J. Sormunen, K. Minkkinen, T. Penttilä, H. Fritze, and E. Tuittila. 2018. Responses of phenology and biomass production of boreal fens to climate warming under different water-table level regimes. Global Change Biology 24:944–956.

Munns, R., and M. Gilliham. 2015. Salinity tolerance of crops —What is the cost? New Phytologist 208:668–673.

Najar, R., S. Aydi, S. Sassi-Aydi, A. Zarai, and C. Abdelly. 2019. Effect of salt stress on photosynthesis and chlorophyll fluorescence in *Medicago truncatula*. Plant Biosystems 153:88–97.

Natali, S. M., E. A. G. Schuur, C. Trucco, C. E. Hicks-Pries, K. G. Crummer, and A. F. BaronLopez. 2011. Effects of experimental warming of air, soil and permafrost on carbon balance in Alaskan tundra. Global Change Biology 17:1394–1407.

Niu, S. L., R. A. Sherry, X. H. Zhou, and Y. Q. Luo. 2013. Ecosystem carbon fluxes in response to warming and clipping in a tallgrass prairie. Ecosystems 16:948–961.

Noyce, G. L., M. L. Kirwan, R. L. Rich, and J. Patrick Megonigal. 2019. Asynchronous nitrogen supply and demand produce nonlinear plant allocation responses to warming and elevated CO$_2$. Proceedings of the National Academy of Sciences USA 116:21623–21628.

Osland, M. J., et al. 2018. Climate and plant controls on soil organic matter in coastal wetlands. Global Change Biology 24:5361–5379.

Reef, R., and C. E. Lovelock. 2014. Regulation of water balance in mangroves. Annals of Botany 115:385–395.

Richardson, A. D., T. F. Keenan, M. Migliavacca, Y. Ryu, O. Sonnentag, and M. Toomey. 2013. Climate change, phenology, and phenological control of vegetation feedbacks to the climate system. Agricultural and Forest Meteorology 169:156–173.

Sun, B. Y., G. X. Han, L. Chen, A. D. Wang, L. X. Wu, and M. Zhao. 2018. Effect of short-term experimental warming on photosynthetic characteristics of *Phragmites australis* in a coastal wetland in the Yellow River Delta, China. Acta Ecologica Sinica 38:167–176.

Wu, Z., P. G. W. Dijkstra, J. P. Koch, and B. A. Hungate. 2011. Responses of terrestrial ecosystems to temperature and precipitation change: a meta-analysis of experimental manipulation. Global Change Biology 17:927–942.

Xia, J. Y., S. L. Niu, and S. Q. Wan. 2009. Response of ecosystem carbon exchange to warming and nitrogen addition during two hydrologically contrasting growing seasons in a temperate steppe. Global Change Biology 15:1544–1556.

Xu, X., Z. Shi, X. Chen, Y. Lin, S. Niu, L. Jiang, R. Luo, and Y. Luo. 2016. Unchanged carbon balance driven by equivalent responses of production and respiration to climate change in a mixed-grass prairie. Global Change Biology 22:1857–1866.

Yao, R. J., and J. S. Yang. 2010. Quantitative evaluation of soil salinity and its spatial distribution using electromagnetic induction method. Agricultural Water Management 97:1961–1970.

Zavaleta, E. S., B. D. Thomas, N. R. Chiariello, G. P. Asner, M. Rebecca Shaw, and C. B. Field. 2003. Plants reverse warming effect on ecosystem water balance. Proceedings of the National Academy of Sciences USA 100:9892–9893.

Zhang, B., W. Li, S. Chen, X. Tan, S. Wang, M. Chen, T. Ren, J. Xia, J. Huang, and X. Han. 2019. Changing precipitation exerts greater influence on soil heterotrophic than autotrophic respiration in a semiarid steppe. Agricultural and Forest Meteorology 271:413–421.

Zhang, L., B. Wang, and L. Qi. 2017. Phylogenetic relatedness, ecological strategy, and stress determine interspecific interactions within a salt marsh community. Aquatic Sciences 79:587–595.

Zhong, Q., Q. Du, J. Gong, C. Zhang, and K. Wang. 2013. Effects of in situ experimental air warming on the soil respiration in a coastal salt marsh reclaimed for agriculture. Plant and Soil 371:487–502.

Zhu, J. T., Y. J. Zhang, and L. Jiang. 2017. Experimental warming drives a seasonal shift of ecosystem carbon exchange in Tibetan alpine meadow. Agricultural and Forest Meteorology 233:242–249.

Zou, J., B. Tobin, Y. Luo, and B. Osborne. 2018. Response of soil respiration and its components to experimental warming and water addition in a temperate Sitka spruce forest ecosystem. Agricultural and Forest Meteorology 260–261:204–215.

SUPPORTING INFORMATION

Additional supporting information may be found in the online version of this article at http://onlinelibrary.wiley.com/doi/10.1002/ecy.3236/suppinfo